Catal Lett (2015) 145:1691–1702
DOI 10.1007/s10562-015-1585-5

Au–Ag/CeO_2 and Au–Cu/CeO_2 Catalysts for Volatile Organic Compounds Oxidation and CO Preferential Oxidation

Roberto Fiorenza[1] · Carmelo Crisafulli[1] · Guglielmo G. Condorelli[1] · Fabio Lupo[1] · Salvatore Scirè[1]

Received: 12 May 2015 / Accepted: 7 July 2015 / Published online: 16 July 2015

Abstract Oxidation of volatile organic compounds (VOC) and preferential oxidation of CO in the excess of H_2 (CO-PROX) were investigated over mono and bimetallic Au–Ag/CeO_2 and Au–Cu/CeO_2 catalysts. For the oxidation of VOC (2-propanol, ethanol and toluene) Au/CeO_2 was the most active catalyst for the combustion of alcohols to CO_2, Ag/CeO_2 gave the best performance in the toluene total oxidation, Au–Ag/CeO_2 and Au–Cu/CeO_2 showed the highest selectivity to partial oxidation products. For CO-PROX Au–Ag/CeO_2 and Au–Cu/CeO_2 samples exhibited higher CO_2 yield at low temperature than monometallic ones. The improved performance of bimetallic catalysts were accounted for an enhancement of surface ceria oxygens mobility caused by the addition of Ag or Cu to Au/CeO_2 and involved in both investigated reactions. This effect was more evident on Au–Ag/CeO_2 where a strong Au–Ag interaction occurred with formation of Au–Ag alloy or linked monometallic nanoparticles.

Graphical Abstract

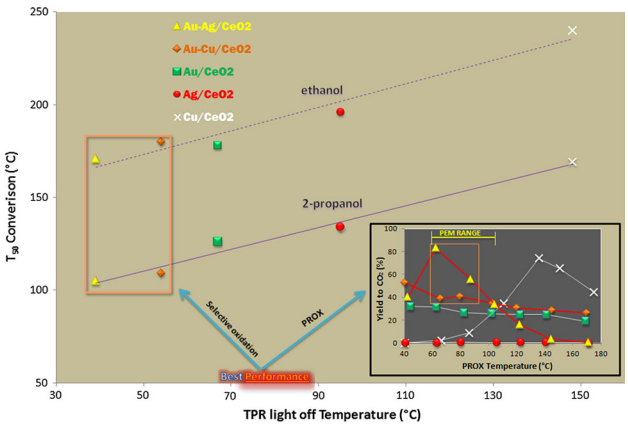

Keywords Gold · Silver · Copper · Bimetallic catalysts · Cerium oxide · VOC · PROX

1 Introduction

Since pioneering works of Haruta [1, 2], research and industrial interest in catalysis by gold extraordinarily increased with an exponential growth in the number of published articles dealing with the use of gold in homogeneous or heterogeneous catalysis. Some of these papers showed that gold properties are much superior to those of the platinum group metals for several reactions such as hydrogenation, selective oxidation of hydrocarbons, alkenes epoxidation, NO_x reduction, water–gas shift reaction, oxidation of volatile organic compounds (VOC) [3–5 and refs. therein].

Electronic supplementary material The online version of this article (doi:10.1007/s10562-015-1585-5) contains supplementary material, which is available to authorized users.

✉ Salvatore Scirè
sscire@unict.it

[1] Dipartimento di Scienze Chimiche, Università di Catania, Viale A. Doria 6, 95125 Catania, Italy

Among the above investigated reactions the oxidation of VOC is a hot environmental topic, VOC being recognized as major responsible for the increase in global air pollution due to their contribution to photochemical smog [6–8]. Catalytic combustion is one of the most efficient technology for the abatement of VOC, which are oxidized over a catalyst at temperatures much lower than those of the thermal process [9–13]. Among noble metal catalysts gold has been reported as one of the most active for this reaction [5]. The performances of Au catalysts for VOC oxidation were dependent on many factors, namely the nature and the properties of the support, the loading, the size, the shape and the electronic state of gold nanoparticles, the preparation method and the pretreatment conditions of catalysts, the nature and the concentration of the organic molecule to be combusted [3–5]. Among catalysts reported in the literature Au/CeO_2 exhibited the highest activity in the oxidation of oxygenated VOC (alcohols, aldehydes, ketones and esters) [5]. This high activity was ascribed to the high surface oxygen mobility of the gold/ceria system, the ceria lattice oxygens being involved in the reaction pathway through a Mars–Van Krevelen (MVK) mechanism [14, 15]. In this contest small gold nanoparticles have been reported to enhance the reactivity of ceria lattice oxygens by weakening the surface Ce–O bonds adjacent to Au atom [16].

Gold supported nanoparticles were also found highly active for the preferential oxidation of CO (CO-PROX) [17, 18], which is aimed at the removal of CO in the excess of hydrogen to obtain pure H_2 for PEM fuel cells (PEMFC). The presence of carbon monoxide in reforming H_2 (1000–10,000 ppm) poisons, in fact, the platinum electrodes of fuel cells. Hence, it is important from a practical point of view to reduce by means of PROX the CO content to less than 10 ppm, without oxidizing H_2, possibly working at the operating temperatures of PEMFC (60–100 °C). Although promising performance can be achieved with monometallic gold catalysts, they suffer from some intrinsic defects that sometimes limit the application of gold systems at high temperature, as strong decrease in the selectivity at temperature higher that 60–80 °C, tendency to aggregation upon heat treatment [19], high sensitivity to moisture [20].

One of the most promising approaches to overcome these problems is the addition of a second metal to gold [21]. Alloying gold with Pd or Pt has proved for instance as an effective method to increase the activity of monometallic systems in selective oxidation reactions [22]. Au–Cu was one of the most investigated bimetallic system with several examples of excellent performance reported both for selective oxidation of 5-hydroxymethylfurfural to 2,5-furandicarboxylicacid [23], for CO oxidation [24] and CO-PROX [25]. Au–Ag catalysts also received considerable attention in the literature for glucose oxidation [26], CO oxidation [27] and CO-PROX [28].

Following these considerations in this paper we investigated the effects of addition of Cu and Ag, with the aim to enlighten the role played by the second metal in affecting the chemico-physical properties and therefore the performance of the monometallic system in the CO-PROX reaction and in the oxidation of some representative VOC (ethanol, 2-propanol and toluene).

2 Experimental

2.1 Catalyst Preparation and Testing

The catalysts were prepared by deposition–precipitation (DP) using KOH as precipitant agent and $HAuCl_4$, $AgNO_3$ and $Cu(NO_3)_2{\cdot}6H_2O$ as precursors of the IB metal for gold, silver and copper respectively.

The cerium oxide used as support was prepared by precipitation from $Ce(NO_3)_3{\cdot}6H_2O$ and calcination in air at 450 °C for 4 h. For Au, Ag and Cu samples after the pH of the aqueous solutions of the IB precursor was adjusted to the value of 8 using an aqueous solution of KOH (0.1 M), cerium oxide was added under vigorous stirring (500 rpm) to the solution, keeping the slurry at 70 °C for 3 h. The obtained slurry was kept digesting for 24 h at room temperature, filtered and washed several times (until disappearance of nitrates and chlorides) then dried at 110 °C and finally ground before use. The same procedures were used for the bimetallic systems ($Au–Ag/CeO_2$ and $Au–Cu/CeO_2$) with the difference that the solution of the second metal was added 30 min after to the addition of cerium oxide at the solution of $HAuCl_4$. All systems were prepared to 1 wt% (for the bimetallic systems 1 wt% Au–1 wt% Ag or Cu). All samples had similar values of surface area ranging between 110 and 118 m^2g^{-1}.

Catalytic tests were carried out in the gas phase at atmospheric pressure in a continuous-flow reactor filled with the catalyst (50 mg, 80–140 mesh) diluted with inert glass powder. For each experiment the reactor temperature was ramped at the rate of 10 °C min^{-1} up to chosen temperature in a flow of helium. Then the reactant mixture was passed over the catalyst for 15 min (to reach a steady-state) before sampling the products for analysis. By using the above procedure, conversion and selectivities were reproducible within 3–5 %.

Preliminary runs carried out at different flow-rates showed the absence of external diffusional limitations. The absence of internal diffusion limitations was verified by running experiments with different grain size powders. We excluded the occurrence of heat transfer limitations, because we found that the temperature of the reactor at

different heights was substantially the same, reasonably due to the low concentration of the reactants used in the catalytic tests.

For VOC oxidations the reactant mixture (0.7 vol% VOC, 10 vol% O_2, balance in helium) was fed to the reactor by flowing a part of the He stream through a saturator containing the VOC and then mixing with O_2 and He before reaching the catalyst. Used VOCs were 2-propanol (Fluka >99.5 %), ethanol (Fluka >99.8 %) and toluene (Fluka >99.5 %). A flow rate of the reactant mixture of 45 ml min^{-1} with a resulting space velocity (GHSV) of 7.6×10^{-3} mol_{VOC} h^{-1} g_{cat}^{-1} was used. The effluent gases were analysed on-line by a gas chromatograph, equipped with a packed column with 10 % FFAP on Chromosorb W and FID detector, and by a quadrupole mass spectrometer (VG quadropoles). The carbon balance was always higher than 95 %. Before VOC oxidation activity tests samples were calcined in air at 200 °C. It must be underlined that 200 °C was chosen as calcination temperature as we verified that a higher temperature leads to a sintering of metal particles with detrimental effect on the activity.

In the case of PROX reaction the gas composition (flow rate: 80 ml min^{-1}) was 1 % CO, 1 % O_2, balance in H_2. A space velocity (GHSV) of 3.92×10^{-2} mol_{CO} h^{-1} g_{cat}^{-1} was used. The effluent gases were analysed on-line by a gas chromatograph, equipped with a packed column (Carboxen 1000) and TCD detector. Before PROX activity tests samples were calcined in air at 200 °C and then reduced in H_2 at 150 °C.

2.2 Catalyst Characterization

Temperature programmed reduction with hydrogen (H_2-TPR) was carried out in a conventional flow apparatus with a TCD detector at heating rate of 10 °C min^{-1} using 5 vol% H_2 in Ar. Before TPR experiments samples were calcined in air at 200 °C.

X-ray photoelectron spectroscopy (XPS) analysis was performed at a take-off angle of 45°, relative to the surface plane, with a PHI 5600 Multi Technique System (base pressure of the main chamber 2×10^{-10} Torr). The spectrometer is equipped with a dual Mg/Al standard X-ray source and a spherical capacitor analyzer (SCA) with a mean diameter of 279.4 mm. The samples were excited with a standard Al Kα radiation. The XPS peak intensities were obtained after Shirley background removal and the binding energy scale was calibrated by centering the C 1 s peak (due to adventitious carbon) at 285.0 eV [29, 30].

X-ray powder diffraction (XRD) analysis was performed with a BrukerAXSD5005 X-ray diffractometer using a Cu Kα radiation. Diffraction peaks of crystalline phases were compared with those of standard compounds reported in the JCPDS Data File.

Surface area measurements were carried out using the BET nitrogen adsorption method with a Sorptomatic series 1990 (Thermo Quest). Before tests all samples were outgassed (10^{-3} Torr) at 120 °C.

TG/DTA measurements were carried out on a Linseis STA PT 1600 instrument. Samples (20.0 ± 0.1 mg) were heated in a aluminum sample boat up to 500 °C at 20 °C/min with a stream of nitrogen gas.

3 Results

3.1 Catalytic Activity

3.1.1 VOC Oxidation

Figure 1 shows the conversion of 2-propanol and the yield to CO_2 and acetone, as a function of reaction temperature on all tested catalysts. Acetone is the first product formed at low temperature with a high selectivity, which decreases down to zero at higher temperatures with a corresponding increase of the selectivity to CO_2. In agreement with literature data [16], the observed order of activity for conversion of 2-propanol for the monometallic samples was $Au/CeO_2 > Ag/CeO_2 > Cu/CeO_2$ with light off temperature of 60 °C for Au/CeO_2, 90 °C for Ag/CeO_2 and 120 °C for Cu/CeO_2. Interestingly both Au–Cu/CeO_2 and Au–Ag/CeO_2 catalysts showed a higher selectivity to the intermediate oxidation product, with a higher yield to acetone compared to monometallic samples. In particular the Au–Ag/CeO_2 sample exhibited the best partial oxidation performance reaching the highest yield to acetone (93 % at 175 °C). It must be noted that the monometallic Au sample remains the most active for the total oxidation to CO_2. This behaviour is better pointed out from data of Table 1, where T_{10}, T_{50}, and T_{90} - conversion values (i.e the temperature at which 10, 50 and 90 % conversion were reached) are reported.

The same catalysts were tested for the oxidation of ethanol and the catalytic results are shown in Fig. 2. It can be noted that the oxidation of ethanol, which is a primary alcohol, required higher temperatures respect to 2-propanol. In this case acetaldehyde is the intermediate product formed firstly. The order of activity for the conversion of ethanol for the monometallic samples was the same than for 2-propanol, ie. $Au/CeO_2 > Ag/CeO_2 > Cu/CeO_2$ with light off temperatures of 95 °C for Au/CeO_2, 100 °C for Ag/CeO_2 and 155 °C for Cu/CeO_2. The performance of the Au–Cu bimetallic catalyst was almost similar to that of monometallic Au/CeO_2 sample, whereas the Au–Ag/CeO_2 sample shows slightly better performance in the selective oxidation to acetaldehyde. For the total oxidation to CO_2 both Au and Ag monometallic samples were the most active (Table 2).

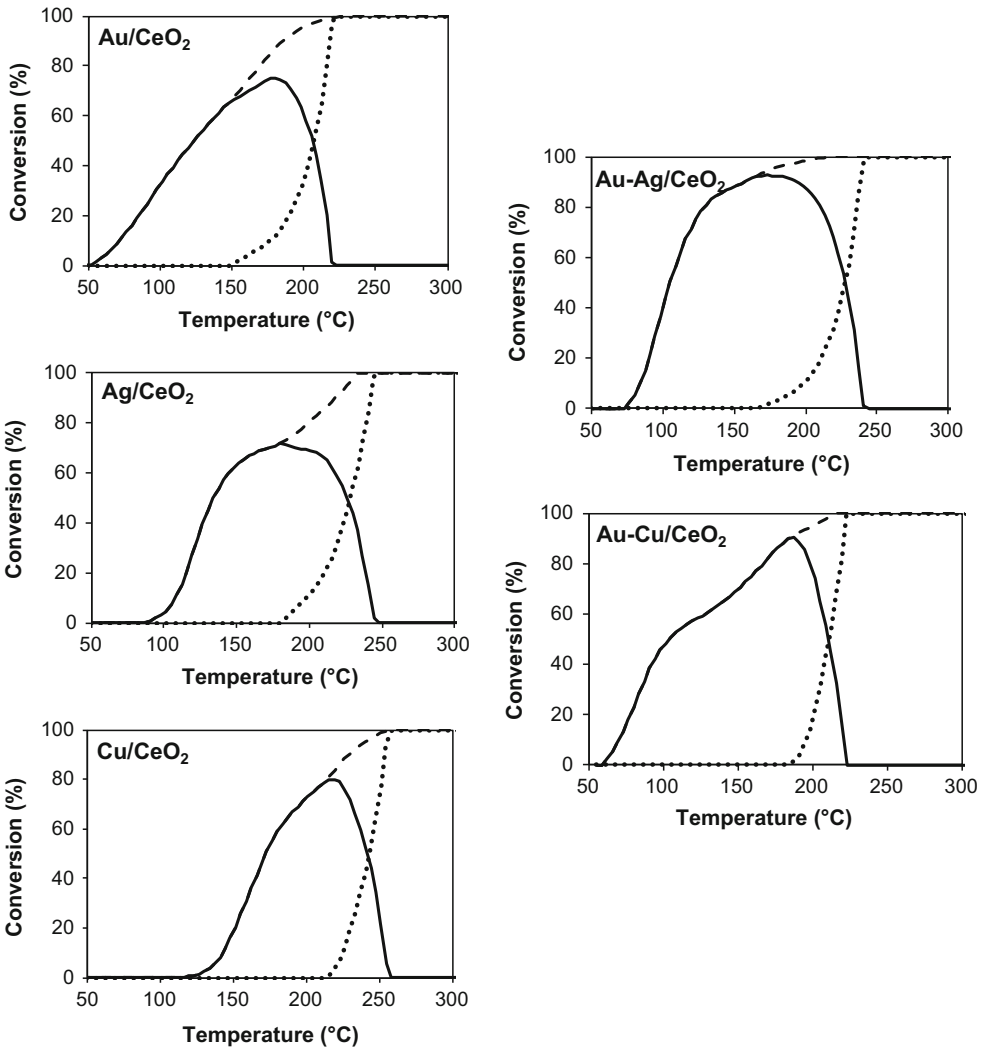

Fig. 1 Conversion of 2-propanol (*dashed lines*) and yield to acetone (*lines*) and to CO_2 (*dotted lines*) on tested samples

Table 1 Catalytic activity data of 2-propanol oxidation

Catalysts	2-Propanol conversion			Conversion to CO_2			Conversion to acetone	
	T_{10} (°C)	T_{50} (°C)	T_{90} (°C)	T_{10} (°C)	T_{50} (°C)	T_{90} (°C)	Max. (%)	T_{max} (°C)
Au/CeO_2	72	126	187	177	207	218	75	180
Ag/CeO_2	108	134	218	198	229	242	72	180
Cu/CeO_2	141	169	229	224	243	252	80	218
$Au–Ag/CeO_2$	84	105	158	199	227	238	93	173
$Au–Cu/CeO_2$	70	109	183	195	210	220	90	187

In Fig. 3 the results of the catalytic oxidation of toluene were reported. In this case, CO_2 and water were the only products revealed, with no formation of intermediate oxidation products, such as benzaldehyde and/or benzoic acid. The absence of partial oxidation compounds has been already reported in the literature under similar experimental conditions over ceria supported catalysts [31] and was attributed to the strong interaction of the acidic intermediates with the basic support, promoting the further oxidation to CO_2. It can be noted that the light-off temperature of toluene over all investigated samples is considerably higher than that observed for 2-propanol and ethanol oxidation, according to the higher reactivity of alcohols compared to aromatics [32, 33]. Interestingly, in this case the monometallic silver catalyst was slightly more active than the monometallic gold one, probably as a consequence of the stronger interaction of aromatic molecules over Ag nanoparticles [34, 35]. In accordance with

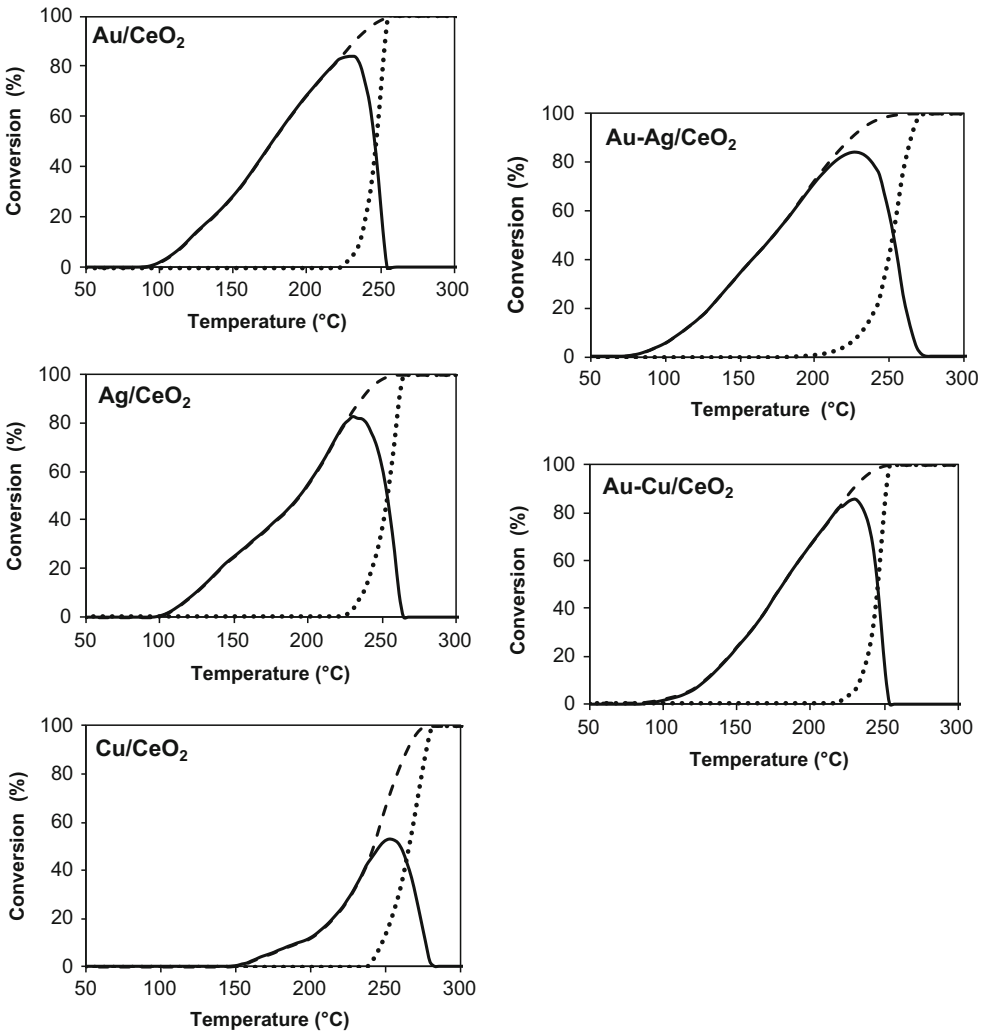

Fig. 2 Conversion of ethanol (*dashed lines*) and yield to acetaldehyde (*lines*) and to CO_2 (*dotted lines*) on tested samples

Table 2 Catalytic activity data of ethanol oxidation

Catalysts	Ethanol conversion			Conversion to CO_2			Conversion to acetaldehyde	
	T_{10} (°C)	T_{50} (°C)	T_{90} (°C)	T_{10} (°C)	T_{50} (°C)	T_{90} (°C)	Max. (%)	T_{max} (°C)
Au/CeO_2	118	178	234	231	246	252	84	230
Ag/CeO_2	124	196	235	237	253	261	82	230
Cu/CeO_2	190	240	261	243	262	273	53	249
Au–Ag/CeO_2	110	171	224	231	253	265	84	228
Au–Cu/CeO_2	128	180	228	234	245	252	85	230

data of total oxidation of alcohols, previously reported, we can suggest that when high temperatures are required for the combustion reaction the activity of Au catalyst decreases becoming similar to that of the silver sample. Both Au–Ag/CeO_2 and Au–Cu/CeO_2 catalysts are less active for the toluene oxidation than monometallic silver and gold samples, confirming that bimetallic samples are less active for the combustion to CO_2, as previously found for the oxidation of alcohols.

3.1.2 CO-PROX Reaction

Figure 4 shows catalytic activity results, in terms of conversion of CO (Fig. 4a) conversion of O_2 (Fig. 4b),

selectivity towards CO oxidation (Fig. 4c) and yield to CO_2 (Fig. 4d) over investigated samples. No methane was formed in all experiments. It must be also reminded that no significant CO and O_2 conversion were observed up to 250 °C on the bare support (CeO_2). From the figure it can be observed that, on all samples, CO conversion (Fig. 4a) increased with increasing reaction temperature reaching a maximum, which was respectively of 70 % for Au/CeO_2 at 60 °C, 95 % for Cu/CeO_2 at 175 °C, 5 % for Ag/CeO_2 at 120 °C, 85 % for Au–Cu/CeO_2 at 80 °C and 95 % for Au–Ag/CeO_2 at 85 °C. These results point out that the CO oxidation activity is strongly affected by the catalytic system, with higher CO conversion values in the PEMFC temperature range (60–100 °C) for the bimetallic samples, Au–Ag/CeO_2 being the most efficient. Noteworthy, the activity of the bimetallic Au–Ag/CeO_2 sample was higher than the sum of the activities of the corresponding monometallics. Over all investigated samples the O_2 conversion (Fig. 4b) continuously increased up to 100 % with reaction temperature then remaining at this value at higher temperatures. Selectivity towards CO oxidation (Fig. 4c), defined as the ratio of O_2 consumption for the CO oxidation to the total O_2 consumption, was always found to decrease on increasing reaction temperature. This behaviour agrees with results reported in the literature and it is attributed to the fact that activation energy of H_2 oxidation was found to be sensibly higher than that of CO oxidation [36, 37]. This behaviour is also in accordance to the finding that on gold and copper particles the ratio of surface coverage between CO and H (θ_{CO}/θ_H) has been found to strongly decrease as temperature increases [38]. It must be also noted that the occurrence of the reverse water gas shift (RWGS) reaction cannot be fully excluded, chiefly at the highest temperatures. However, according to the literature, the RWGS should take place only at reaction temperatures higher than those employed in our experiments. In fact, no RWGS reaction was reported to occur on copper supported on ceria catalysts by Marino et al. at temperatures lower than 200 °C with a conversion to CO of only 1.1 % reached at 300 °C [39]. It is also important to remind that, according to results reported in the literature [35], at the

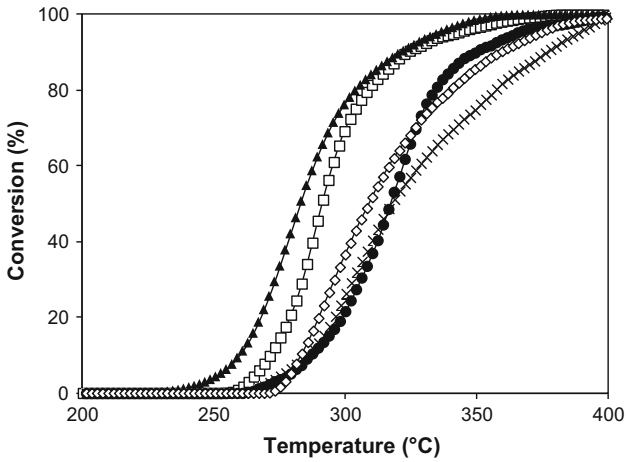

Fig. 3 Conversion of toluene on tested samples: (*open square*) Au/CeO_2; (*filled triangle*) Ag/CeO_2; (*times*) Cu/CeO_2; (*open diamond*) Au–Cu/CeO_2; (*filled circle*) Au–Ag/CeO_2

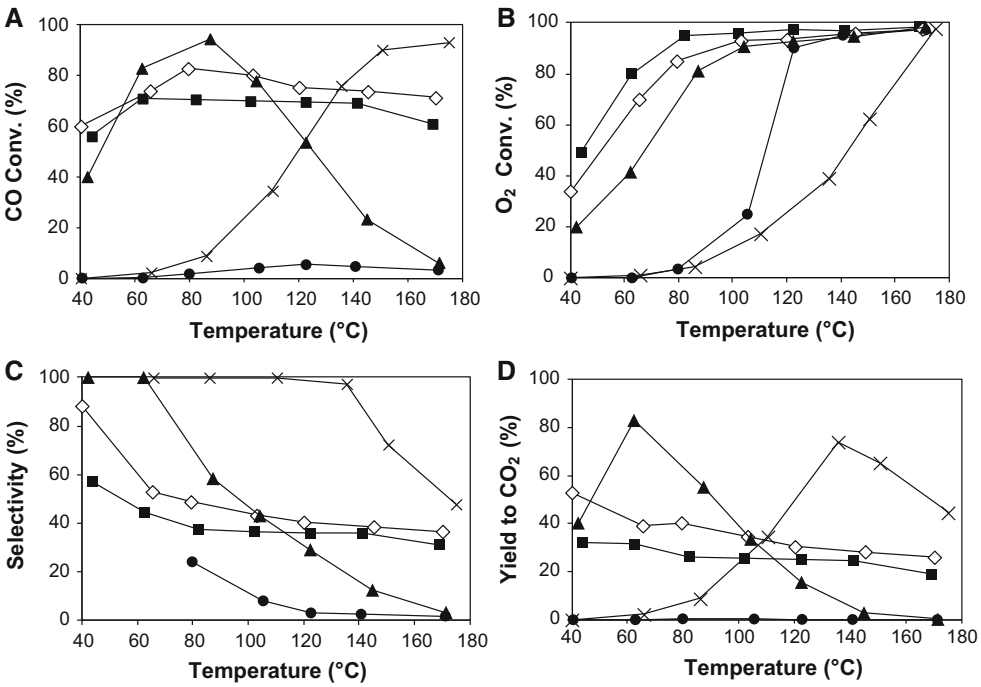

Fig. 4 PROX activity data: **a** CO conversion, **b** O_2 conversion, **c** selectivity towards CO oxidation and **d** yield to CO_2 over tested samples. (*Filled square*) Au/CeO_2; (*times*) Cu/CeO_2; (*filled circle*) Ag/CeO_2; (*open diamond*) Au–Cu/CeO_2; (*filled triangle*) Au–Ag/CeO_2

same reaction temperature, selectivity was roughly independent from the level of conversion. It is noteworthy that the rate of decrease of selectivity as a function of the temperature strongly depends on the catalytic system used. In fact, on Au/CeO_2 the selectivity (57 % at around 40 °C) decreases since low temperature (~40 °C), whereas on Cu/CeO_2 it remained around 100 % up to 110 °C then gradually decreasing at higher temperatures. On Ag/CeO_2 the selectivity was always very low (<20 %), decreasing in any case with reaction temperature. The Au–Cu/CeO_2 catalyst exhibited slightly better performance compared to Au/CeO_2 sample with a higher selectivity (85 %) at 40 °C and a similar decreases at high temperatures. The Au–Ag/CeO_2 showed 100 % selectivity at low temperature and a rapid drop for T > 60 °C. Data reported in Fig. 4d clearly point out that Au–Ag/CeO_2 was the most active system for CO oxidation to CO_2 at low temperature, whereas the Au–Cu/CeO_2 showed slightly better performance compared to Au monometallic sample. The Cu/CeO_2 sample was the most effective at higher temperature whereas Ag/CeO_2 was always a bad PROX catalyst.

3.2 Catalysts Characterization

3.2.1 H_2-TPR Results

Figure 5 reports temperature programmed reduction (H_2-TPR) profiles carried out on ceria based catalysts. In the examined temperature range (30–550 °C) the CeO_2 sample showed one broad reduction peak near 500 °C due to the reduction of the surface capping oxygens of ceria [40]. The reduction of bulk oxygens of ceria does not appear in the TPR profile of Fig. 5, occurring at T > 700 °C [41]. This reduction peak has been reported to be affected by the presence of noble or transition metals [31, 42].

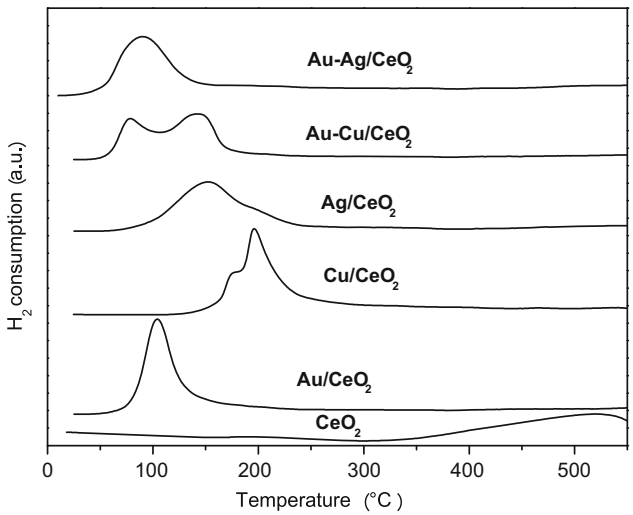

Fig. 5 TPR profiles of investigated catalysts

On Au/CeO_2 a quite symmetric peak centred a 105 °C can be observed. Considering that gold is mainly present in the metallic state, as confirmed by XPS reported in the next paragraph, this peak was attributed to the reduction of ceria surface oxygen species, which in this case occurs at much lower temperature. This shift reflects the ability of highly dispersed gold to weaken the Ce–O bond, thus increasing the mobility of the lattice oxygens [43]. We must remind that the occurrence of spillover phenomena have been reported over gold/ceria and gold/ceria-mixed oxides [44, 45]. This could justify the higher hydrogen consumption observed on Au/CeO_2 compared to the bare CeO_2 (see also Table S1, where a quantitative evaluation of the H_2 consumption is reported).

On Ag/CeO_2 TPR profile exhibited a peak with a maximum at around 150 °C. Taking into account that XPS data pointed to the presence of metallic silver, this reduction peak can be assigned to the reduction of surface capping oxygens of ceria interacting with silver [46]. The higher temperature of this reduction compared to that of the Au/CeO_2 sample indicates a lower interaction of Ag with the ceria support.

The Cu/CeO_2 sample shows a peak with a maximum in the range 190–210 °C and a shoulder at lower temperature (around 180–190 °C). According to the literature [47, 48] and taking into account the H_2 consumption data reported in Table S1, the two features here observed can be attributed to the reduction of CuO clusters and of the surface capping oxygens of ceria that occurs in the same temperature range, making difficult to discriminate between the two components. It is possible to suggest that a mutual interaction between ceria and copper oxide takes place, resulting in an easier reduction of both ceria and copper oxides. In fact the reduction of bulk CuO has been reported to occur at higher temperatures [16, 48, 49].

The Au–Cu/CeO_2 system shows two not well resolved peaks with maxima at 78 °C and 142 °C, both at much lower temperature than those of the monometallic Cu one, suggesting that on the bimetallic system the reduction is assisted by the presence of Au. It has been reported that Au promotes the hydrogen adsorption which subsequently becomes involved in the reduction of both CuO and CeO_2 [25]. In the case of Au–Ag/CeO_2 catalyst, the maximum of peak was found at significantly lower temperature (85 °C) than on all other investigated samples, which implies a stronger interaction of one or both metals (Au and/or Ag) with the support thus improving the mobility/reducibility of surface CeO_2 oxygens.

3.2.2 XPS Results

In order to investigate the oxidation states of involved species (Ce, Au, Ag and Cu), XPS measurements of mono

and bimetallic catalysts were carried out, analyzing Ce 3d, Au 4f, Ag 3d and Cu 2p signals, respectively.

Figure 6 shows the XPS spectra in Ce 3d region for all samples. According to the literature the satellite peak at about 917 eV is the fingerprint of Ce^{4+} state [50] and its high intensity suggests that most part of ceria is in Ce^{4+} oxidation state. The shoulder at around 885 eV indicates also the presence of Ce^{3+} ions. Therefore in all sample both Ce^{4+} and Ce^{3+} species appear to coexist [51].

The analysis of XPS spectra of gold containing catalysts in the Au 4f region are plotted in Fig. 7. Two broad bands are well visible, with maxima at about 84.7 eV (Au $4f_{7/2}$) and 88.4 eV (Au $4f_{5/2}$) respectively for Au/CeO_2 and Au–Cu/CeO_2 catalysts. Interestingly the signals for the Au–Ag/CeO_2 catalyst are shifted to lower BE respectively at 87.8 eV $4f_{5/2}$ and at 84.1 eV for Au $4f_{7/2}$. A shift to lower BE in XPS is usually associated with an increased electron density or a reduction to a lower valence state. Therefore XPS results suggest an electron transfer leading to an increased electron density around the gold [28]. Moreover the signals are more intense respect to Au and Au–Cu samples. In fact, as reported on Table 3, the surface concentration of gold on Au–Ag/CeO_2 catalyst is about three times respect to both Au/CeO_2 and Au–Cu/CeO_2 catalysts.

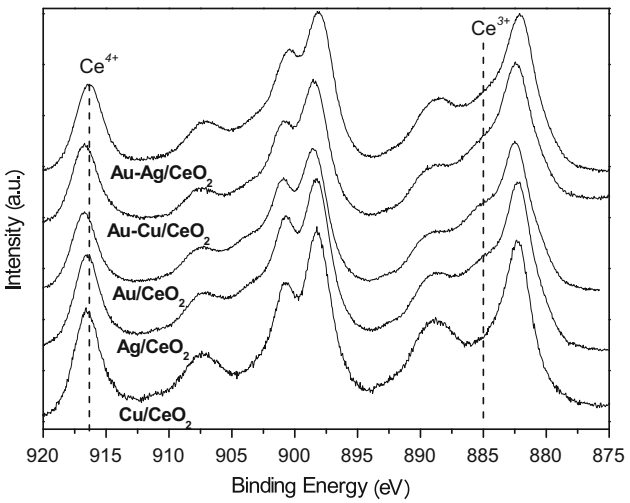

Fig. 6 XPS spectra in the Ce 3d XPS spectra of mono and bimetallic catalysts

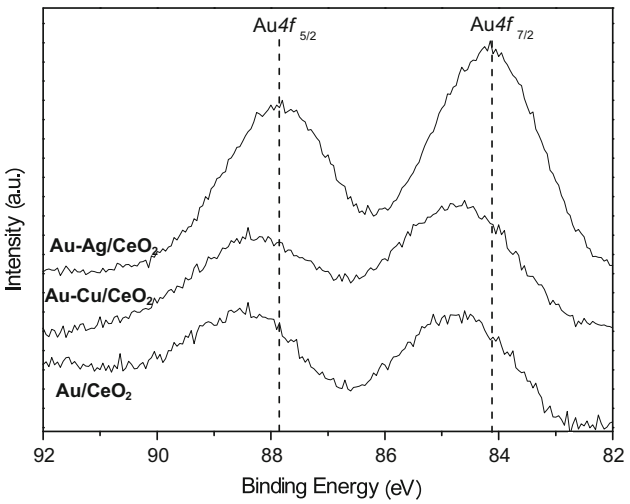

Fig. 7 XPS spectra in the Cu 2p region for Cu/CeO_2 and Au–Cu/CeO_2 catalysts

It has been generally reported that Au^0 species give transitions at 84.0 eV and 87.7 eV whereas higher BE have been reported for oxidized Au species ($Au^{\delta+}$, Au^+ and Au^{3+}) [52]. Therefore, on the basis of the position and the broadness of the bands it can be inferred that gold is mostly present on the catalytic surface as Au° with some oxidized Au species (Fig. 7).

In the case of Ag and Au–Ag catalysts the XPS spectra show two signals (Fig. 8), These bands are located at around 374.0 eV ($Ag3d_{5/2}$) and 368.2 eV for Ag/CeO_2, at 374.0 eV (Ag $3d_{3/2}$) and 368.1 eV for Au–Ag/CeO_2 This indicate the presence of metallic silver [53].

The Cu 2p core level spectra for Cu and Au–Cu catalysts are shown in Fig. 9. The most intense feature is the Cu $2p_{3/2}$ peak, observable at around 932.5 eV for Cu/CeO_2 and at about 932.8 eV for Au–Cu/CeO_2. Both Cu^{+1} and Cu^0 contributed to the Cu $2p_{3/2}$ peak, but it is difficult to solve the individual contribution of each of them. The Cu monometallic sample showed a shoulder at about 943 eV that can be attributed to the presence of traces of Cu^{2+} [47].

The surface compositions of investigated catalysts, calculated on the basis of XPS analysis, are summarized in Table 3. On the monometallic samples the surface concentration of the active metal was 0.2, 0.8 and 1.7 wt% for Au, Ag and Cu, respectively. Considering that the bulk metal composition of all monometallic samples was 1 wt%, the above values point to a significant surface copper enrichment in the case of Cu/CeO_2, as already reported in the literature [25]. On the contrary on Au/CeO_2 the concentration of gold is much lower than the bulk one suggesting that Au is partially buried into the ceria support [31]. Interestingly, the bimetallic Au–Cu/CeO_2 exhibited a surface composition similar to that of the corresponding monometallic samples, with a resulting Cu/Au surface ratio of 7.5. This implies a low degree of Au–Cu interaction, as also pointed out by TPR analysis. In contrast in the Au–Ag/CeO_2 sample the surface composition is quite different from that of the corresponding monometallic samples with a strong enrichment in Au and a moderate impoverishment in Ag, resulting in a Ag/Au surface ratio of 1.08, quite near to the bulk one. This is compatible with the formation of a Au–Ag alloy or linked monometallic nanoparticles [28, 54].

Table 3 Surface composition of samples estimated by XPS

Catalysts	Au (wt%)	Ag (wt%)	Cu (wt%)	Cu/Au or Ag/Au ratio
Au/CeO_2	0.2	–	–	–
Ag/CeO_2	–	0.8	–	–
Cu/CeO_2	–	–	1.7	–
$Au–Ag/CeO_2$	0.6	0.65	–	1.08
$Au–Cu/CeO_2$	0.2	–	1.5	7.5

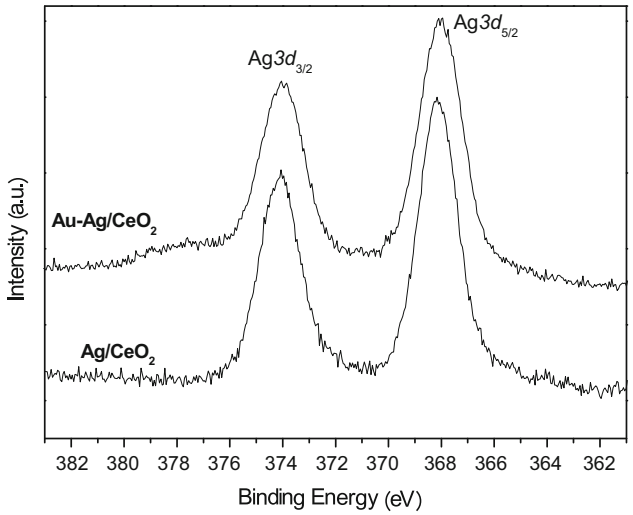

Fig. 8 XPS spectra in the Ag 3d region for Ag/CeO_2 and Au–Ag/CeO_2 catalysts

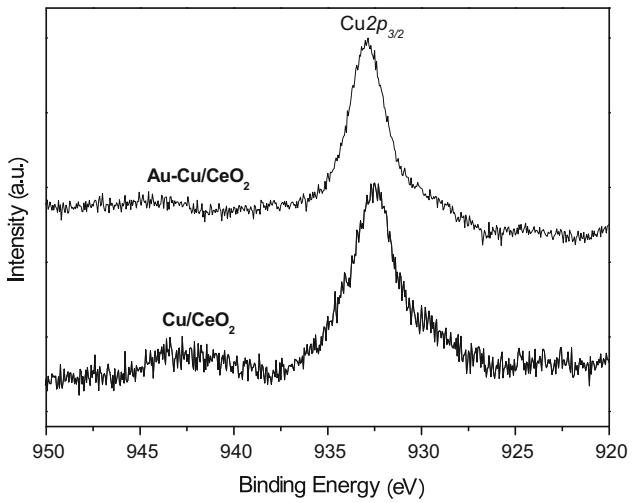

Fig. 9 XPS spectra in the Au 4f region for Au/CeO_2, Au–Ag/CeO_2 and Au–Cu/CeO_2 catalysts

3.2.3 TG/DTA Analysis

The TG and DTA curves of all investigated catalysts are reported in Fig. 10. The samples show small weight losses (<3 %) in the 100–200 °C range (Fig. 10a) attributed to

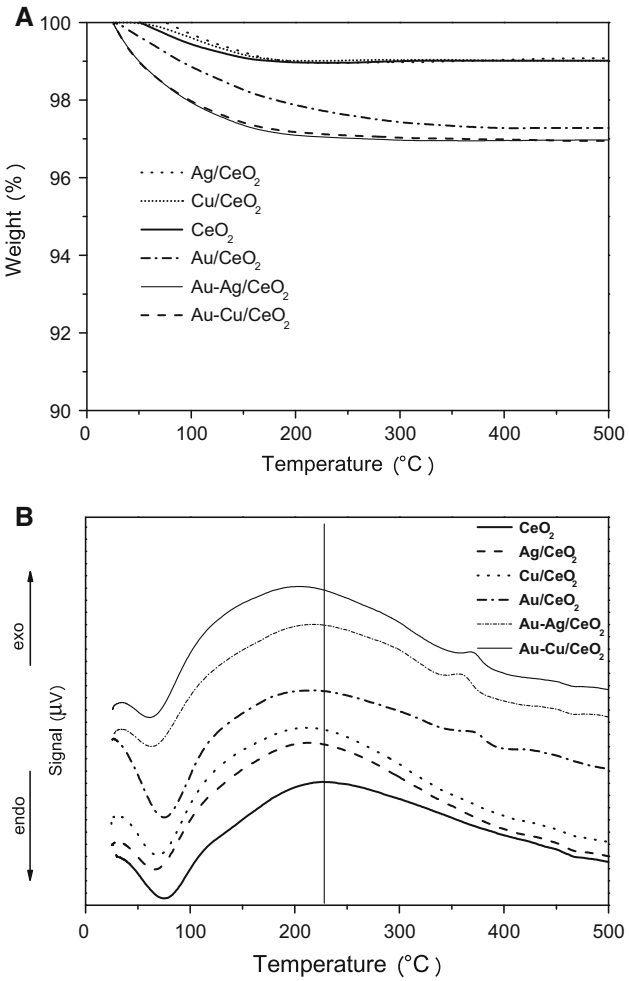

Fig. 10 **a** TG and **b** DTA profiles of investigated catalysts

the desorption of physisorbed water molecules as confirmed by the endothermic peak visible in the DTA profiles (Fig. 10b). No weight loss was then observed up to 500 °C, while DTA showed an exothermic peak with a maximum at 200–230 °C, which can be assigned to the crystallization of amorphous portion of cerium oxide [55, 56]. Interestingly this conformational transition was observed at 230 °C on pure ceria shifting to lower temperatures when a metal is deposited on the support, reasonably due to the introduction of major defects in the crystalline structure of ceria. Another exothermic feature can be observed in the 340–390 °C range only in the Au containing samples

(mono and bimetallic) and it has been attributed to the decomposition of residual chlorides from the precursor used ($HAuCl_4$) [57].

4 Discussion

Data reported in the present paper showed that the addition of copper or silver strongly affects the catalytic behaviour of the Au/CeO_2 system both for VOC oxidation and CO-PROX reaction.

In the case of VOC oxidation $Au–Ag/CeO_2$ and $Au–Cu/CeO_2$ bimetallic samples exhibited higher activity than monometallic Au/CeO_2 towards the oxidation of 2-propanol to acetone and, to a less extent, ethanol to acetaldehyde. A synergistic effect between Au and Cu or Ag, that results in an improvement of the selective oxidation of alcohols, has been reported in the literature [58, 59]. The deep oxidation of the alcohols to CO_2 was instead inhibited by the presence of the second metal. A negative role of the addition of Ag or Cu to Au/CeO_2 was also found in the oxidation of toluene. This is quite reasonable considering that over ceria supported gold catalysts toluene oxidation has been reported to proceed directly to CO_2, without formation of intermediate oxidation products [5]. These results clearly points out that $Au–Ag/CeO_2$ and $Au–Cu/CeO_2$ systems are suitable for the selective oxidation of alcohols to the corresponding carbonyl compound (ketone or aldehyde), whereas the monometallic Au/CeO_2 is the best catalyst for the combustion of oxygenated VOC.

In the preferential oxidation of CO, which can be regarded as a selective oxidation reaction where the CO molecule must be selectively oxidized in the presence of an excess of hydrogen, the addition of Ag to Au/CeO_2 also results in an evident improvement of the catalytic performance. In fact, $Au–Ag/CeO_2$ strongly enhanced the low temperature (60–100 °C) CO conversion with respect to the H_2 one, thus leading to a much higher yield to CO_2 and then to a better efficiency in the low temperature CO removal from H_2 rich streams, namely under reaction conditions adopted in PEMFC applications. A similar, but less evident, positive effect was observed in the case of the bimetallic $Au–Cu/CeO_2$ sample. Some examples of synergism between gold and copper or silver, giving superior performance respect to the corresponding monometallic gold catalyst have been reported in the literature [25, 27, 54, 60]. Sandoval et al. stated that the synergistic effect between Au and Ag supported on TiO_2 results in significantly higher activity in CO oxidation and better stability than the monometallic gold catalyst [27]. Déronzier et al. observed a strong interaction between gold and silver, that resulted in a higher CO oxidation selectivity at low temperature, ascribed to a large segregation of silver inhibiting the H_2 adsorption [54]. Liao et al. highlighted that the synergistic effect between Au and Cu over ceria was highly dependent upon the Cu/Au atomic ratio and the thermal treatment, with the best performance obtained over reduced catalysts, due to a decrease in the amount of surface copper species upon reduction treatments [25]. Finally Liu et al. reported an enhancement in the catalytic activity of silica supported Au–Cu bimetallic catalysts for both CO oxidation and PROX reaction, taking place mainly at high reaction temperatures ($T \approx 200$ °C) [60].

In order to explain the better performance of investigated bimetallic Au based catalysts in selective oxidations it must be taken into account that the oxidation of VOC over reducible oxides based catalysts has been reported to strongly depend on the mobility of lattice oxygen of the oxide, as in this case of ceria [31, 61]. However it has been suggested that chemisorbed and lattice oxygens are both involved, with a comparable effect, in the deep oxidation of VOC to CO_2, whereas the selective oxidation is mainly affected by lattice oxygens of metal oxides [12, 62]. Effectively in our case, H_2-TPR profiles (Fig. 5) pointed out that all IB metals (Au, Ag or Cu) deposited on CeO_2 promote the reducibility of ceria lattice oxygen species, which directly reflects the mobility/reactivity of these oxygens [12, 14]. This effect was more pronounced for bimetallic Au–Ag and Au–Cu samples, being the highest for $Au–Ag/CeO_2$. As reported in the literature [63] the improvement in low-temperature reducibility should be beneficial for catalytic activity both of VOC oxidation and CO-PROX reactions which have been reported to occur through a MVK redox mechanism [5, 13, 64–66]. Interestingly, as shown in Fig. 11, a good correlation has been found to exist between the temperature at which the reduction of the catalyst began to occur (TPR initial

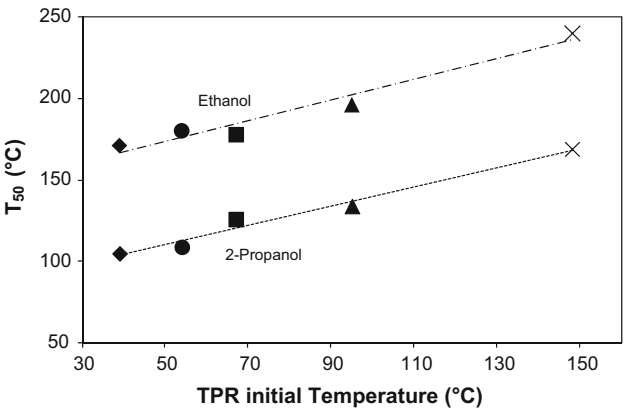

Fig. 11 T_{50} ethanol and 2-propanol conversions versus TPR initial temperature: (*filled diamond*) $Au–Ag/CeO_2$; (*filled circle*) $Au–Cu/CeO_2$; (*filled square*) Au/CeO_2; (*filled triangle*) Ag/CeO_2; (*times*) Cu/CeO_2

Table 4 Activity of catalysts in the PROX reaction at 60 °C

Catalysts	Yield to CO_2(%)	CO conversion (%)
Au–Ag/CeO_2	81	83
Au–Cu/CeO_2	38	74
Au/CeO_2	30	70
Ag/CeO_2	0	0
Cu/CeO_2	2	2

temperature) and the temperature at which 50 % of alcohols conversion was reached (at this temperature the oxidation proceeds almost selectively to intermediate products as shown in Figs. 1 and 2). Data of Fig. 11 show that Au–Ag/CeO_2 and Au–Cu/CeO_2 are at the same time more reducible and more active towards the selective oxidation than monometallic Au/CeO_2. The same activity trend was also found in the CO-PROX as shown in Table 4, where CO conversion and yield to CO_2 are summarized. The above results support the hypothesis that the mobility of ceria surface oxygens is crucial for the activity in the selective oxidation reaction [12, 62]. The increase in the lattice oxygen mobility of ceria observed by addition of Ag or Cu to Au/CeO_2 is probably a consequence of a higher disorder of the ceria lattice induced by metals, as also suggested by TG–DTA measurements [67]. It must be underlined that all investigated samples exhibited comparable values of surface area (110–118 m^2g^{-1}), ruling out that the higher reducibility can be somehow ascribed to a higher surface area.

The better performance in the selective oxidation of alcohols and in the CO-PROX of the Au–Ag/CeO_2 catalyst with respect to Au–Cu/CeO_2 can be accounted for the different surface metal composition of investigated samples. In fact, XPS data (Table 3) showed that in the case of the Au–Cu bimetallic catalyst the surface concentration of gold and copper was similar to that of the corresponding monometallic Au and Cu samples and then richer in copper (present as both Cu^{+1} and Cu^0) than in gold (present mostly as Au^0). This surface composition was in accordance with the low Au–Cu interaction suggested by TPR. On the Au–Ag/CeO_2 sample, instead, the surface gold and silver compositions were quite different from those of the monometallic samples with a Au enrichment and a Ag impoverishment. It can be reasonably suggested that in the Au–Ag/CeO_2 bimetallic sample a strong Au–Ag interaction (formation of a stoichiometric Ag–Au alloy or linked monometallic particles) occurs, promoting the dispersion of gold and enhancing the catalytic performance [28, 54]. Sasirekha et al. proposed that the occurrence of this strong interaction between Au–Ag boosted the performance of the PROX reaction by increasing the stability of catalysts [28].

Unfortunately in our case it was not possible to verify the alloy formation by XRD, mono and bimetallic catalysts showing only the fluorite structure of CeO_2 without peaks related to Au or Ag (see Fig. S1 in supplementary information), probably due to the fact that either gold and silver particles were too small or too low in amount and size to be detected by XRD. In fact, the preparation method employed (DP with KOH) leads to Au particles smaller than 5 nm [4, 5, 13]. Moreover the presence of silver or copper reported to hinder the Au sintering at high temperatures [21, 27, 51]. On the basis of the above consideration we can reasonably suggest that the occurrence of a strong Au–Ag interaction, with formation of Au–Ag alloy or bimetallic clusters, is able to promote a major enhancement of surface ceria oxygens mobility which positively affects partial oxidation reactions more than deep combustion ones.

5 Conclusions

On the basis of the results reported in the present paper the following conclusions can be drawn, providing some new insights into the field of VOC oxidation and CO-PROX reactions:

- Au–Ag/CeO_2 and Au–Cu/CeO_2 bimetallic samples showed a higher selectivity to intermediates in the oxidation of alcohols (in our case acetone from 2-propanol and acetaldehyde from ethanol), making these systems good candidates for selective oxidation reactions.
- Au/CeO_2 was the most active catalyst for the deep oxidation of alcohols to CO_2, confirming the superior performance of this system for the combustion of oxygenated VOC.
- Ag/CeO_2 gave better performance than Au/CeO_2 in the deep oxidation of toluene to CO_2, making this catalyst interesting from a practical point of view for the toluene combustion, also in consideration of the lower cost of silver compared to gold.
- In the PROX reaction Au–Ag/CeO_2 and Au–Cu/CeO_2 bimetallic samples showed higher CO conversion and yield to CO_2 at low temperatures (<100 °C) than the monometallic Au/CeO_2 sample, being suitable for application in the purification of H_2 for PEMFC.
- The addition of Ag or Cu to Au/CeO_2 causes an enhancement of surface ceria oxygens mobility, leading to higher activity towards preferential oxidation of CO and selective oxidation of VOC, reported to occur through a MVK mechanism. This synergistic effect was more evident on Au–Ag/CeO_2 where a stronger interaction between Au and Ag has been found to occur.

References

1. Haruta M, Kobayashi T, Sano H, Yamada N (1987) Chem Lett 16:405
2. Haruta M, Yamada N, Kobayashi T, Iijima S (1989) J Catal 115:301
3. Freakley SJ, He Q, Kiely CJ, Hutchings GJ (2015) Catal Lett 145:71
4. Hashmi ASK, Rudolph M (2008) Chem Soc Rev 37:1766
5. Scirè S, Liotta LF (2012) Appl Catal B 125:222
6. Heck RM, Farrauto RJ (2002) Catalytic pollution control, Second edn. Wiley, New York
7. Amann M, Lutz M (2000) J Hazard Mater 78:41
8. Atkinson R (2000) Atmos Environ 34:2063
9. Li WB, Wang JX, Gong H (2009) Catal Today 148:81
10. Ojala S, Pitkaaho S, Laitinen T, Koivikko NN, Brahmi R, Gaalova J, Matejova L, Kucherov A, Paivarinta S, Hirschmann C, Nevanpera T, Riihimaki M, Pirila M, Keiski RL (2011) Top Catal 54:1224
11. Papaefthimiou P, Ioannides T, Verykios XE (1997) Appl Catal B 13:175
12. Spivey JJ (1987) Ind Eng Chem Res 26:2165
13. Liotta LF (2010) Appl Catal B 100:403
14. Scirè S, Minicò S, Crisafulli C, Galvagno S (2000) Appl Catal B 28:245
15. Milone C, Ingoglia R, Pistone A, Neri G, Galvagno S (2003) Catal Lett 87:201
16. Scirè S, Riccobene PM, Crisafulli C (2010) Appl Catal B 101:109
17. Haruta M (1997) Catal Today 36:153
18. Haruta M, Tsubota S, Kobayashi T, Kageyama M, Genet MJ, Delmon B (1993) J Catal 144:175
19. Bell AT (2003) Science 299:1688
20. Daté M, Okumura M, Tsubota S, Haruta M (2004) Angew Chem Int Ed 43:2129
21. Wang A, Liu XY, Mou CY, Zhang T (2013) J Catal 308:258
22. Bianchi CL, Canton P, Dimitratos N, Porta F, Prati L (2005) Catal Today 102–103:203
23. Albonetti S, Lolli A, Morandi V, Migliori A, Lucarelli C, Cavani F (2015) Appl Catal B 163:520
24. Nikolaev SA, Golubina EV, Krotova IN, Shilina MI, Chistyakov AV, Kriventsov VV (2015) Appl Catal B 168–169:303
25. Liao X, Chu W, Dai X, Pitchon V (2013) Appl Catal B 142–143:25
26. Benkó T, Beck A, Frey K, Srankó DF, Geszti O, Sáfrán G, Maróti B, Schay Z (2014) Appl Catal A 479:103
27. Sandoval A, Aguilar A, Louis C, Traverse A, Zanella R (2011) J Catal 281:40
28. Sasirekha N, Sangeetha P, Chen YW (2014) J Phys Chem C 118:15226
29. Swift P (1982) Surf Interface Anal 4:47
30. Briggs D, Beamson G (1992) Anal Chem 64:1729
31. Scirè S, Minicò S, Crisafulli C, Satriano C, Pistone A (2003) Appl Catal B 40:43
32. O'Malley A, Hodnett BK (1999) Catal Today 54:31
33. Baldi M, Finocchio E, Milella F, Busca G (1998) Appl Catal B 16:43
34. Won Baek S, Kim JR, Ihm SK (2004) Catal Today 93–95:575
35. Qua Z, Bua Y, Qina Y, Wanga Y, Fub Q (2013) Appl Catal B 132–133:353
36. Scirè S, Crisafulli C, Minicò S, Condorelli GG, Di Mauro A (2008) J Mol Catal A 284:24
37. Kahlich MJ, Gasteiger HA, Behm RJ (1999) J Catal 182:430
38. Kandoi S, Gokhale AA, Grabow LC, Dumesic JA, Mavrikakis M (2004) Catal Lett 93:93
39. Marino F, Descorme C, Duprez D (2008) Appl Catal B 58:175
40. Yao HC, Yao YF (1984) J Catal 86:254
41. Trovarelli A, Dolcetti G, De Leitenburg C, Kaspar J, Finetti P, Santoni A (1992) J Chem Soc, Faraday Trans 88:1311
42. Tabakova T, Bocuzzi F, Manzoli M, Sobczak JW, Idakiev V, Andreeva A (2006) Appl Catal A 298:127
43. Andreeva D, Idakiev V, Tabakova T, Ilieva L, Falaras P, Bourlinos A, Travlos A (2002) Catal Today 72:51
44. Wang X, Perret N, Delgado JJ, Blanco G, Chen X, Olmos CM, Bernal S, Keane MA (2013) J Phys Chem C 117:994
45. Meng M, Tu Y, Ding T, Sun Z, Zhang L (2011) Int J Hydrogen Energy 36:9139
46. Kundakovic LJ, Flytzani-Stephanopoulos M (1998) Appl Catal A 171:13
47. Avgouropoulos G, Ioannides T (2003) Appl Catal A 244:155
48. Luo MF, Zhong YJ, Yuan XX, Zheng XM (1997) Appl Catal A 162:121
49. Fierro G, Jacono ML, Inversi M, Porta P, Lavecchia R, Cioci F (1994) J Catal 148:709
50. Beche E, Charvin P, Perarnau D, Abanades S, Flamant G (2008) Surf Interface Anal 40:264
51. Gamboa-Rosales NK, Ayastuy JL, Gonzalez-Marcos MP, Gutierrez-Ortiz MA (2012) Int. J Hydrogen Energy 37:7005
52. Venezia AM, Pantaleo G, Longo A, Di Carlo G, Casaletto MP, Liotta L, Deganello G (2005) J Phys Chem B 109:2821
53. Moulder JF, Stickle WF, Sobol PE, Bomben KD (1993) Handbook of X-ray photoelectron spectroscopy. Perkin-Elmer Corporation, Eden Prairie
54. Déronzier T, Morfin F, Lomello M, Rousset JL (2014) J Catal 311:221
55. Suresh R, Ponnuswamy V, Mariappan R (2014) Mater Sci Semicond Process 21:45
56. Dos Santos ML, Lima RC, Riccardi CS, Tranquilin RL, Bueno PR, Varela JA, Longo E (2008) Mater Lett 62:4509
57. Otto K, Oja Acik I, Krunks M, Tõnsuaadu K, Mere A (2014) J Therm Anal Calorim 118:1065
58. Li W, Wang A, Liu X, Zhang T (2012) Appl Catal A 433–434:146
59. Huang X, Wang X, Tan M, Zou X, Ding W, Lu X (2013) Appl Catal A 467:407
60. Liu X, Wang A, Zhang T, Su DS, Mou CY (2011) Catal Today 160:103
61. Trovarelli A, Fornasiero P (2014) Catalysis by ceria and related materials, Second edn. Imperial College Press, London
62. Pearce R, Patterson WR (1981) Catalysis and chemical processes. Wiley, New York
63. Liu B, Liu Y, Li C, Hu W, Jing P, Wang Q, Zhang J (2012) Appl Catal B 127:47
64. Andreeva D, Petrova P, Sobczak JW, Ilieva L, Abrashev M (2006) Appl Catal B 67:237
65. Mars P, Van Krevelen DW (1954) Chem Eng Sci (Spec Suppl) 3:41
66. Doornkamp C, Ponec V (2000) J Mol Catal A 162:19
67. Neri G, Visco AM, Galvagno S, Donato A, Panzalorto M (1999) Thermochim Acta 329:39